Comparison of Gas-Phase and Solution-Phase Reactions of Dimethyl Sulfide and 2-(Methylthio)ethanol with Hydroxyl Radical

Michael L. McKee

Department of Chemistry, Auburn University, Auburn, Alabama 36849

Received: March 18, 2003; In Final Form: May 18, 2003

The reaction of the OH radical with dimethyl sulfide (DMS) and 2-(methylthio)ethanol (2-MTE) proceeds with the initial formation of a two-center−three-electron complex. In the gas phase the S−OH binding enthalpies (298 K) are 8.7 and 12.2 kcal/mol for DMS and 2-MTE, respectively. When entropy and aqueous solvation effects (via the CPCM method) are included, the free energies of association (298 K) of hydroxyl to DMS and 2-MTE become 3.0 and 3.2 kcal/mol, respectively. Calculations are based on DFT and/or MP2 optimizations and a G2-like method for evaluating energies. The most favorable (lowest free energy) conformation is often different between the gas phase and solution phase. Electron transfer from 2-MTE/2-MTE$^+$ (**1**/**1**$^+$) to OH/OH$^-$ has a positive free energy of 4.5 kcal/mol and is in competition with the acid-/base-catalyzed formation of $CH_3SCH_2CH_2O$ (**2**) plus water. The latter radical (**2**) undergoes intramolecular hydrogen transfer to form $CH_2SCH_2CH_2OH$ (**3**) or eliminates formaldehyde to form CH_2SCH_3+H_2C═O, where the free energy barriers are 7.9 and 8.3 kcal/mol, respectively. The 2-MTE cation (**1**$^+$) can eliminate a C−H proton to form three different radicals that are within 2.0 kcal/mol of each other in free energy.

1. Introduction

The oxidation of sulfides by hydroxyl radical is an important process in the gas phase[1−8] and in solution.[9−22] Dimethyl sulfide in the atmosphere is thought to undergo oxidation by the initial addition of the hydroxyl radical to form a two-center−three-electron (2c−3e) adduct that reacts with molecular oxygen to form DMSO plus peroxyl radical (eqs 1 and 2).

$$SMe_2 + OH \rightleftarrows HO\therefore SMe_2 \quad (1)$$

$$HO\therefore SMe_2 + O_2 \rightarrow DMSO + O_2H \quad (2)$$

The aqueous-phase oxidation of organic sulfides by hydroxyl radical has been the subject of many investigations. Asmus and co-workers[9] have generated hydroxyl radicals by γ-radiolysis. The reaction with sulfides is complex, but a major pathway is the formation of the $2\sigma/1\sigma^*$ 2c−3e radical cation (eqs 3 and 4).

$$SR_2 + \bullet OH \rightarrow HO\therefore SR_2 \quad (3)$$

$$HO\therefore SR_2 + SR_2 \rightarrow R_2S\therefore SR_2^+ + OH^- \quad (4)$$

Schöneich and co-workers[14−22] have used pulse radiolysis to generate hydroxyl radicals to investigate the effect of oxygen free radicals in a biological environment. Hydroxyl radicals have been implicated in the damage of DNA and tRNA.

An investigation of the reactivity of 2-MTE (2-(methylthio)-ethanol)) with hydroxyl radical was undertaken due to the broad interest in one-electron oxidation of organic sulfides. Specifically, 2-MTE has been used as a model for a protein with the methionine residue (Met side chain = $CH_3SCH_2CH_2$) that may be oxidized upon exposure to reactive oxygen species such as the hydroxyl radical.

SCHEME 1: Possible Reactions of 2-MTE with Hydroxyl Radical in Solution Phase

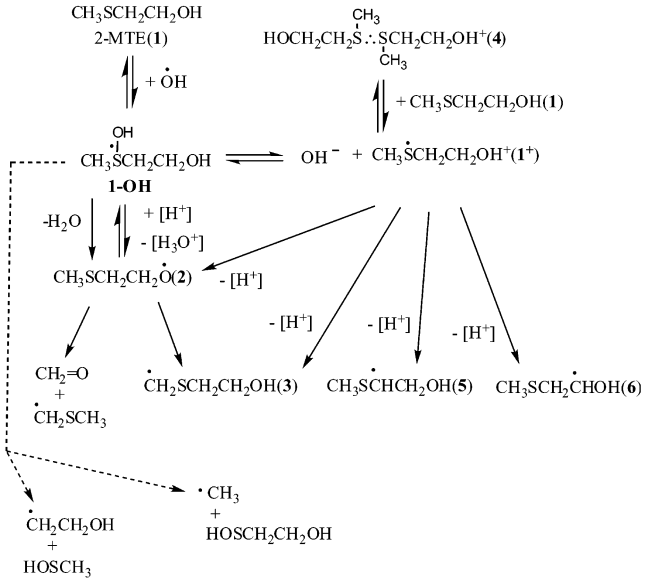

Mittal[10,11] carried out pulse radiolysis experiments and monitored absorption spectra of OH-adducts and/or dimer radical cations. Schöneich and co-workers[14−22] used laser flash photolysis and steady-state photolysis experiments. In the latter experiments, the yield of formaldehyde was determined by derivatization. The general reaction scheme is given in Scheme 1. The fragmentation of the OH-adduct $CH_3S(OH)CH_2CH_2OH$ to CH_3 + $HOSCH_2CH_2OH$ or CH_2CH_2OH + CH_3SOH has not been considered previously. However, it should be noted that the thermodynamically favored fragments in the gas-phase reaction of OH with DMSO is CH_3 + $CH_3S(O)OH$.[23]

10.1021/jp034704h CCC: $25.00
Published on Web 08/09/2003

TABLE 1: Absolute Energies (hartees), Zero-Point Energies, Heat Capacity Corrections, Entropies, and Free Energies of Solvation at the B3LYP/6-31+G(d) Level

	B3LYP/6-31+G(d)	ZPE[a]	Cp corr[b]	S[c]	CPCM[d,e]	exptl[f]
OH	−75.733 50	5.21	2.07	42.61	−3.59	−2.0[h]
OH^-	−75.796 68	5.23	2.07	41.20	−108.25	−103.1[i]
H_2O	−76.422 57	13.24	2.37	45.12	−3.00[g]	−2.05
H_3O^+	−76.691 52	21.52	2.41	46.21	−105.45	−108.3[i]
CH_2SCH_3	−477.357 91	38.79	3.81	71.12	0.35	
$H_2C{=}O$	−114.508 84	16.79	2.39	52.25	0.48	
CH_3	−39.842 64	18.76	2.51	46.54	3.45	
CH_2CH_2OH	−154.374 33	40.90	3.41	66.42	−4.83	
$HOSCH_3$	−513.901 22	32.65	3.42	67.42	−4.61	
$HOSCH_2CH_2OH$	−628.432 23	54.33	4.51	78.11	−8.52	
$HOSCH_2CH_2OH'$	−628.425 80	53.81	4.95	83.53	−11.64	
1 (2-MTE)	−592.547 35	69.08	4.93	81.89	−4.59	
1-OH	−668.310 36	77.30	6.04	91.16	−7.59 (−7.31)	
1-OH (MP2)		77.88	5.68	88.49	−2.98 (−1.28)	
TS1-OH/2·H_2O	−668.290 80	73.32	5.87	90.06	−7.80 (−5.58)	
TS1-OH/2·H_2O (MP2)		73.64	5.72	88.65	−7.84 (−9.95)	
2	−591.879 37	59.81	4.91	83.38	−3.49	
2·H_2O	−668.308 10	75.36	6.95	100.17	−4.51	
$\mathbf{1}^+$	−592.239 19	68.64	5.08	84.74	−52.77	
$\mathbf{1}^{+\prime}$	−592.235 62	68.12	5.22	86.05	−59.65	
$\mathbf{1}^+$·H_2O	−668.680 19	83.62	7.16	104.05	−49.61	
TS2/3	−591.866 19	57.97	3.99	75.47	−3.47	
3	−591.887 25	60.59	4.77	81.03	−3.81	
3′	−591.884 92	60.04	5.15	84.21	−6.65	
4 (S∴S)	−1184.835 36	138.97	10.63	134.10	−44.70	
5	−591.887 13	60.41	5.11	85.15	−6.02	
6	−591.888 35	60.34	5.06	83.86	−6.78	
TS2/$H_2C{=}O$	−591.863 48	58.36	5.06	85.29	−3.31	
1-OH·H_2O	−744.746 26	93.11	7.70	104.42	−7.80	
TS1-OH·H_2O/2 + $2H_2O$	−744.719 25	88.61	7.27	101.87	−9.42	
TS1-OH/CH_3	−668.258 39	75.62	6.06	91.94	−1.27	
TS1-OH/CH_3′	−668.252 54	75.28	6.36	95.59	−9.39	
TS1-OH/CH_2CH_2OH	−668.261 45	75.71	6.07	93.24	−6.94	
DMS	−478.017 74	47.75	3.66	67.88	0.56 (1.50)	
DMS (MP2)		47.79	3.62	67.46	0.53 (1.42)	
DMS-OH	−553.773 05	55.25	5.22	83.52	−3.74 (−0.53)	
DMS-OH (MP2)		55.80	4.94	82.05	1.84 (5.17)	
$\mathbf{DMS}^+$	−477.700 22	46.81	3.94	73.77	−51.98	
DMS∴$\mathbf{DMS}^+$	−955.768 19	96.55	7.83	105.60	−39.09	

[a] Zero-point energies in kcal/mol. [b] Heat capacity corrections to 298 K. B3LYP/6-31+G(d) frequencies are used for all structures except those marked with "MP2", where MP2/6-31+G(2d) frequencies were used. [c] Entropies in cal/mol K. B3LYP/6-31+G(d) frequencies are used for all structures except those marked with "MP2", where MP2/6-31+G(2d) frequencies were used. [d] The free energy of hydration was computed at the CPCM/B3LYP/6-31+G(d)//B3LYP/6-31+G(d) level using a dielectric constant of 78.39. A correction factor of 1.90 kcal/mol was added to the calculated values to account for the change of state from 1 mol/atm (24.47 L at 298 K in gas phase) to 1 mol/L (aqueous phase). The values in parentheses were computed at the CPCM/MP2/6-31+G(d) level. [e] In G98 the solvation free energy (ΔG(solv)) at the DFT level is directly printed (electrostatic plus nonelectrostatic term). The MP2 solvation energy was computed by taking the difference in the UMP2 electronic energy in the gas-phase and solution-phase and adding the nonelectrostatic term. [f] Mallard, W. G.; Linstrom, P. J., Eds. *NIST Chemistry WebBook*; NIST Standard Reference Database Number 69, February 2000, National Institute of Standards and Technology: Gaithersburg, MD, 2000 (http://webbook.nist.gov) [g] An additional correction factor of 2.38 kcal/mol was added to account for the change in state from 1 mol/L (aqueous phase) to 55.5 mol/L (liquid). [h] See the text. [i] Zhan and Dixon have computed the free energy of hydration for OH^- (−104.5 kcal/mol)[46] and H_3O^+ (−107.15 kcal/mol).[45]

2. Computational Method

All calculations used the Gaussian98 program system.[24] The density functional theory exchange/correlation combination B3/LYP has been used with the 6-31+G(d) basis set for geometry optimization. This level of theory has proven to be effective in reproducing geometries in a wide variety of bonding environments.[25] In fact, the accuracy of B3LYP has been found to be roughly the same as CCSD when comparing geometries and frequencies for radical species.[26] Vibrational frequencies have been computed at the B3LYP/6-31+G(d) level to confirm the nature of the stationary points and to make zero-point corrections. The imaginary frequency (transition vector) was animated graphically[27] for all transition states to ensure that the motion was appropriate for converting reactants to products. Single-point calculations (Table S1) have been made at the QCISD(T)/6-31+G(d) and MP2/6-311+G(3df,2p) levels and combined with the additivity approximation[28] to estimate relative energies at the [QCISD(T)/6-311+G(3df,2p)] level (eq 5).

$$\Delta E(\text{QCISD(T)/6-311+G(3df,2p)}) \approx \Delta E(\text{QCISD(T)/6-31+G(d)}) + \Delta E(\text{MP2/6-311+G(3df,2p)}) - \Delta E(\text{MP2/6-31+G(d)}) \quad (5)$$

The approximation in eq 5 is similar to the one used in the G2(MP2,SVP) procedure,[29] except that geometries and zero-point energies (unscaled) are calculated at B3LYP/6-31+G(d) rather than MP2/6-31G(d) (for geometry) and HF/6-31G(d) (for frequencies). The same higher level correction term (ΔHLC) used for the G2(MP2,SVP) procedure has been included. Thus, the target calculation [QCISD(T)/6-311+G(3df,2p)] is similar to the G2(MP2,SVP) method, which has been shown by Radom

TABLE 2: Relative Energies, Enthalpies, and Free Energies (Gas-Phase and Solution-Phase) in kcal/mol at the B3LYP/6-31+G(d) and WF-1 Levels

	B3LYP/6-31+G(d)[a]				WF-1[b]			
	ΔE(g)	ΔH(g,298K)	ΔG(g,298K)	ΔG(aq,298K)	ΔE(g)	ΔH(g,298K)	ΔG(g,298K)	ΔG(aq,298K)
1 + OH	18.5	16.5	6.5	7.5	14.2	12.2	2.2	3.2
1-OH	0.0	0.0	0.0	0.0	0.0	0.0	0.0	0.0
1-OH (MP2)					−0.1	0.1	0.9	7.2
TS1-OH/2·H_2O	12.3	8.1	8.5	8.2	21.6	17.4	17.7	17.5
TS1-OH/2·H_2O (MP2)					20.2	16.2	16.9	14.6
2·$\mathbf{H_2O}$	1.4	0.4	−2.3	0.8	−0.l	−1.2	−3.8	−0.8
2 + H_2O	5.3	2.3	−8.9	−6.8	3.8	0.8	−10.3	−8.3
TS2/$\mathbf{H_2C{=}O}$ + H_2O	15.3	10.9	−0.8	1.5	14.5	10.2	−1.5	0.8
CH_2SCH_3 + $H_2C{=}O$ + H_2O	13.2	7.3	−15.8	−9.4	10.9	5.0	−18.1	−11.7
TS2/3 + H_2O	13.6	7.8	−1.0	1.1	11.2	5.4	−3.4	−1.3
3 + H_2O	0.3	−2.0	−12.5	−10.7	−8.5	−10.9	−21.3	−19.6
3′ + H_2O	1.8	−0.7	−12.1	−13.2				
TS1-OH/$\mathbf{CH_3}$	32.7	31.0	30.7	37.0				
TS1-OH/$\mathbf{CH_3}$′	36.3	34.6	33.3	31.5				
CH_3 + $HOSCH_2CH_2OH$	22.3	19.0	9.1	11.6	18.4	15.2	5.2	7.7
CH_3 + $HOSCH_2CH_2OH$′	26.3	23.0	11.4	10.8	22.2	18.9	7.3	6.7
TS1-OH/$\mathbf{CH_2CH_2OH}$	30.7	29.1	28.5	29.2				
CH_2CH_2OH + $HOSCH_3$	21.8	18.9	6.2	4.3	20.7	17.7	5.0	3.1
$\mathbf{1}^+$ + OH^-	172.2	169.9	159.6	9.9				
$\mathbf{1}^{+\prime}$ + OH^-	174.5	171.8	161.0	4.5				
5 + H_2O	0.4	−1.8	−13.5	−13.9				
6 + H_2O	−0.4	−2.7	−14.0	−15.2				
1-OH + H_3O^+	0.0	0.0	0.0	0.0				
$\mathbf{1}^+$·$\mathbf{H_2O}$ + H_2O	−63.3	−64.2	−67.7	−4.7				
$\mathbf{1}^+$ + $2H_2O$	−51.7	−54.1	−65.3	−7.5				
$\mathbf{1}^{+\prime}$ + $2H_2O$	−49.5	−52.2	−63.8	−12.8				
1 + $\mathbf{1}^{+\prime}$	0.0	0.0	0.0	0.0				
4 (S∴S)	−32.9	−30.6	−20.5	−1.0				
1-OH + H_2O	0.0	0.0	0.0	0.0				
1-OH·$\mathbf{H_2O}$	−8.4	−6.5	3.0	4.8				
TS1-OH·$\mathbf{H_2O/2}$ + $2H_2O$	8.6	5.5	15.8	16.0				
2 + $2H_2O$	5.3	2.3	−8.9	−6.8				
$\mathbf{1}^{+\prime}$ + H_2O	0.0	0.0	0.0	0.0				
2 + H_3O^+	54.8	54.5	55.0	6.0				
3 + H_3O^+	49.8	50.2	51.3	2.1				
3′ + H_3O^+	51.3	51.5	51.7	−0.4				
5 + H_3O^+	49.9	50.4	50.4	−1.1				
6 + H_3O^+	49.1	49.5	49.5	−2.4				
DMS + OH	13.7	11.9	3.9	6.2	10.5	8.7	0.7	3.0
DMS-OH	0.0	0.0	0.0	0.0	0.0	0.0	0.0	0.0
DMS-OH (MP2)					0.0	0.3	0.7	6.3
DMS + $\mathbf{DMS}^+$	0.0	0.0	0.0	0.0				
DMS∴$\mathbf{DMS}^+$	−31.5	−29.3[c]	−18.5	−6.2				
$\mathbf{DMS}^+$ + $2H_2O$	0.0	0.0	0.0	0.0				
DMS-OH + H_3O^+	50.7	53.1	63.3	8.5				
1 → $\mathbf{1}^+$	193.4	193.1	192.2	144.1				
DMS → $\mathbf{DMS}^+$	199.2	198.6	196.8	144.3				

[a] The energies are at the B3LYP/6-31+G(d)//B3LYP/6-31+G(d) level. The zero-point corrections, temperature corrections, and entropies are computed from unscaled B3LYP/6-31+G(d) frequencies. Solvation free energies are computed at the CPCM/B3LYP/6-31+G(d)//B3LYP/6-31+G(d) level. [b] The energies are from the additivity approximation (eq 5), where B3LYP/6-31+G(d) geometries are used except for entries with "MP2" in the notation, in which cases MP2/6-31+G(2d) geometries are used. The zero-point corrections, temperature corrections, and entropies are computed from unscaled B3LYP/6-31+G(d) frequencies except for entries with "MP2" in the notation, in which cases MP2/6-31+G(2d) frequencies are used. Solvation free energies are computed at the CPCM/B3LYP/6-31+G(d)//B3LYP/6-31+G(d) level. [c] The experimental enthalpy is −27.5 kcal/mol. Reference 57.

and co-workers[29] to reproduce a number of molecular properties to within chemical accuracy (2 kcal/mol). However, it should be pointed out that for transition states and systems with significant spin contamination, the errors may be larger. This level of theory will be denoted WF-1 (wave function level 1).

For several of the species considered, geometries and frequencies were calculated at the MP2/6-31+G(2d) level (rather than the B3LYP/6-31+G(d) level). Since density functional theory is known to be defective in describing the spin/charge localization in 2c−3e bonded systems,[30−37] it was deemed prudent to compare B3LYP and MP2 geometries for the HO/DMS and HO/2-MTE adducts. Solvation effects in water (ϵ = 78.39) were accounted for at the CPCM/B3LYP/6-31+G(d) or CPCM/MP2/6-31+G(d) level of theory (Table 1).[38−42] Unless otherwise noted, solvation calculations were performed on fixed gas-phase geometries. Solution-phase free energies at 298 K ($\Delta G°$(aq)) were computed from eq 6

$$\Delta G°(\mathrm{aq}) = \Delta H(\mathrm{g}) - T\Delta S(\mathrm{g}) + \Delta G(\mathrm{solv}) \qquad (6)$$

where ΔH(g) and ΔS(g) are computed at the B3LYP/6-31+G(d) or WF-1 levels (ΔH(g) corrected for temperature effects to 298 K) and ΔG(solv) is the CPCM value with the electrostatic and nonelectrostatic terms. A correction factor[43,44] of 1.90 kcal/mol (RT ln(24.47)) has been included to account for a change of state from 1 mol/24.47 L (gaseous at 298 K) to 1 mol/L

SCHEME 2: Theromdynamic Cycle Used To Determine ΔG(solv) of H_3O^+

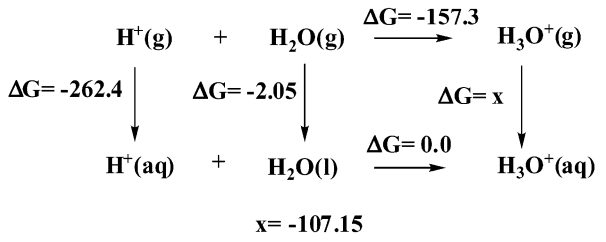

(aqueous). For H_2O(l), there is an additional correction factor of 2.38 kcal/mol for the change of state from 1 mol/L (aqueous phase) to 55.5 mol/L (liquid). Relative energies, enthalpies, and free energies (gas and solution) are given in Table 2 for various species.

Modern computational methods can predict gas-phase reaction energies to within 1 or 2 kcal/mol for systems of the size considered in this study. Unfortunately, the accuracy of solution-phase reactions energies is usually less. Free energies of solvation for neutral and charges species can differ by over 100 kcal/mol. Accurately calculating differences in free energies of solvation is still a challenge for computational methods.

For the solvation free energies (ΔG(solv)) of H_2O(l), H_3O^+(aq), OH^-(aq), and OH(aq) species, the experimental (OH, H_2O) or high-level theory (H_3O^+, OH^-) values were used. The calculated ΔG(solv) for H_2O in mol/atm is -7.28 kcal/mol. Using the correction factor for mol/24.47 L $\rightarrow$ mol/L and the change of state (aq $\rightarrow$ l), the value for ΔG(solv,H_2O(l)) is -3.0 kcal/mol, close to the experimental value of -2.05 kcal/mol. The experimental values for ΔG(solv) of H^+(aq) range from -265 to -251 kcal/mol. There have been several recent quantum mechanical studies of the absolute free energy of H^+(aq) due to the central role this value plays in solution-phase acidities. The recent value of -262.4 kcal/mol calculated by Zhan and Dixon[45] is combined with their proton affinity of H_2O (157.3 kcal/mol) to give a value of -107.15 kcal/mol (Scheme 2) for the solvation free energy of H_3O^+(aq). The CPCM/B3LYP/6-31+G(d) value, -105.45 kcal/mol, is in good agreement. Zhan and Dixon[46] have calculated the free energy of solvation for OH^-(aq) to be -104.5 kcal/mol, somewhat smaller than the calculated value of -108.25 kcal/mol. From the $\Delta G°_f$ of OH^-(aq) and OH(g) (-37.6 and 8.2 kcal/mol, respectively)[47] and the OH^-/OH redox couple (1.90 eV),[48] a value of -2.0 kcal/mol is derived for ΔG(solv) of OH(aq).[49] This value can be compared with the calculated value of -3.6 kcal/mol (CPCM/B3LYP/6-31+G(d)). The free energies of solvation were also computed for several species at the CPCM/ MP2/6-31+G(d)//MP2/6-31+G(2d) level. In general, the MP2 solvation free energies are about 1−2 kcal/mol more positive than the B3LYP values (Table 1).

The "standard" WF-1 energies are computed at B3LYP/6-31+G(d) geometries and using DFT frequencies to compute thermodynamic properties and/or at MP2/6-31+G(2d) geometries with MP2 frequencies (Tables 1 and 2). While it is inconsistent to use different methods to compute geometries, zero-point energies, and heat capacity corrections, in practice the two methods give very similar results. In the case of Me(R)SOH, R = Me, CH_2CH_2OH, the DFT and MP2 zero-point energies were within 0.5 kcal/mol of each other and the heat capacity corrections within 0.3 kcal/mol.

Cartesian coordinates of all species in Table 1 are available as Supporting Information (Table S2). Molecular structures at the B3LYP/6-31+G(d) level are shown for species on the 2-MTE/OH potential energy surface in Figure 1 where numerical values are enthalpies (298K) at the WF-1 level relative to the 2-MTE/OH adduct.

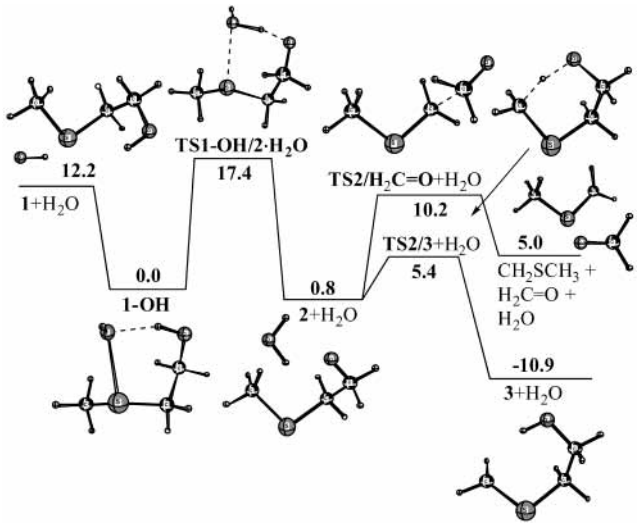

Figure 1. Reaction coordinate for OH + 2-MTE where values are enthalpies (298 K) at the WF-1 level of theory. All structures were optimized at the B3LYP/6-31+G(d) level.

3. Results and Discussion

The theoretical description of the Me_2S−OH adduct has proven to be quite challenging.[50−54] Wine and co-workers[7] have used laser flash photolysis-induced fluorescence (LFP-LIF) to determine a gas-phase binding enthalpy (298K) of 13.0 kcal/mol. Tureček[51] calculated a binding enthalpy (298 K) of 9.6 kcal/mol for eq 1 using the [QCISD(T)/6-311++G(3df,2p)]//B3LYP/6-31++G(2d,p)+ZPC+Cp method, where the square brackets indicate the use of the additivity approximation which is close to the WF-1 value of 8.7 kcal/mol (Table 2).

Initially, the complex was believed to involve a hydrogen bond between OH and Me_2S, since that was the only minimum that could be found at the MP2/6-31G(d) level.[53,54] However, when the MP2 method was used with a larger basis set for geometry optimization (MP2/6-31+G(2d)), a weak coordination (S−O distance about 2 Å) was found between oxygen and sulfur that is best described as a 2c−3e interaction.[50] Symmetrical 2c−3e complexes such as $X\therefore X^-$ (X = F, Cl, Br, I) and $R_2S\therefore SR_2^+$ are well-known and have unpaired electron density equally distributed over two centers. Of the three resonance structures, $X\therefore X \leftrightarrow X^+X^- \leftrightarrow X^-X^+$, the first one dominates. For unsymmetrical 2c−3e interactions, the localization of spin and charge are important factors in describing the interaction. Unfortunately, wave function and density functional theory have difficulty in describing the relative contribution of the three resonance structures $X\therefore Y \leftrightarrow X^+Y^- \leftrightarrow X^-Y^+$ in unsymmetrical complexes.[55−57] Wave function theory tends to overestimate charge/spin localization, while density functional theory tends to underestimate charge/spin localization. At the MP2/6-31+G(2d) level the S−O bond is 2.047 Å, much shorter than the 2.353 Å distance found with B3LYP/6-31+G(d).[58] A study[59] of the reaction coordinate for addition of OH to the sulfur atom of CS_2 found that the UMP2 method significantly underestimates the interaction energy (too unstable) between S−O distances of about 2.0−2.4 Å compared to QCISD(T), while B3LYP overestimates the interaction energy (too stable).[31] Thus, neither method (DFT or MP2) seems to be ideally suited for computing the S−O bond in Me_2S−OH. In the gas phase, the results are

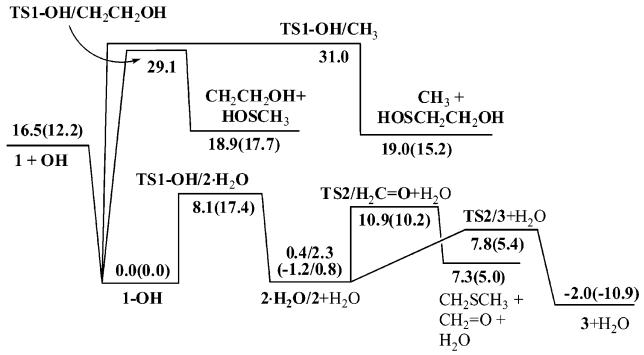

Figure 2. Reaction coordinate for OH + 2-MTE with enthalpies (298 K) at the B3LYP/6-31+G(d) level with WF-1 values in parentheses. Two values are given for **2**·H_2O/**2** + H_2O. The first corresponds to the complex between **2** and water and the second corresponds to **2** plus H_2O.

not very sensitive to the method used for computing the geometry. At the WF-1//B3LYP/ 6-31+G(d) level the OH binding enthalpy (298 K) is 8.7 kcal/mol, which is reduced to 8.4 kcal/mol at the WF-1//MP2/6-31+G(2d) level. This suggests that the optimized S∴O distance at the QCISD(T)/6-311+G(3df,2p) level is closer to the DFT value than to the MP2 value.[58]

Since the Me_2S-OH complex has been characterized in aqueous solution, it is of interest to compute solution-phase properties. Solvation effects will favor a more localized charge distribution with $Me_2S^+-OH^-$ polarity. The solvation free energies are significantly more negative at the DFT-optimized Me_2S-OH geometry (−3.74 kcal/mol, Table 1) compared to the MP2-optimized geometry (−0.53 kcal/mol), which is due to the greater charge separation in the DFT geometry (dipole moments = 5.33(2.72) D by DFT(MP2)). Optimizing at the CPCM/B3LYP/6-31+G(d) level lowers the electronic energy by only 0.4 kcal/mol. Geometry optimization could not be carried out at the CPCM/MP2 level because gradients are not available at that level.

Reaction of 2-(Methylthio)ethanol (2-MTE) with OH.

The conformational surface of 2-MTE was partially explored. Unless otherwise noted, the conformer displayed is the lowest energy found. Solvation free energies were computed at fixed gas-phase geometries. In almost every case, a different conformer was preferred in the gas and solution phases. While the lowest energy gas-phase structure was characterized by an internal hydrogen bond, solution effects favored a more extended conformation. If the lowest energy gas-phase and solution-phase conformers are different, an apostrophe was added to the label of the aqueous phase conformer. The discussion below will be divided into two parts, gas phase and solution phase.

Gas Phase. Marstokk et al.[60] studied the microwave spectrum of 2-MTE (**1**) and concluded that the all-gauche conformer was lowest in energy. The same conformer was found to be lowest in energy in the present study. However, there is little intramolecular hydrogen bonding between the OH hydrogen and sulfur as judged by the H−S separation of 2.675 Å.[61]

The geometry of the OH-adduct (**1-OH**, Figure 1) was optimized with DFT and MP2. Similar to the Me_2S-OH adduct, the S−O distance in **1-OH** is much longer at the DFT level (2.381 Å) than the MP2 level (2.087 Å). When energies at both geometries are evaluated at the WF-1 level, the computed bond enthalpy (298 K) is very similar (12.2 kcal/mol at the DFT geometry and 12.1 kcal/mol at the MP2 geometry). The DFT OH binding enthalpy (16.5 kcal/mol) is probably somewhat overestimated (Figure 2).

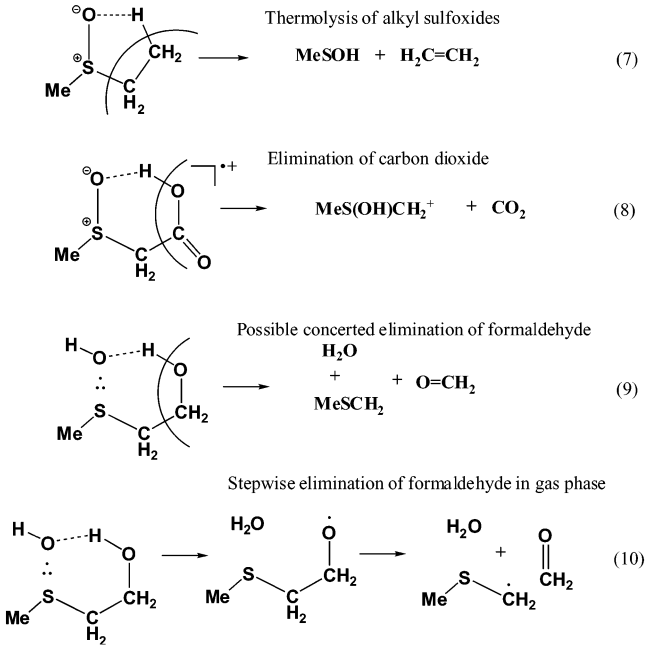

Figure 3. Depiction of the relationship between elimination of ethylene from alkyl sulfoxides (eq 7), elimination of carbon dioxide from methyl carboxylmethyl sulfoxide radical cation (eq 8), and elimination of formaldehyde from the OH adduct with 2-MTE (eq 9). Equation 7 is computed[63] to be concerted while eq 9 is computed to be stepwise (eq 10).

The OH binding enthalpy in **1-OH** is significantly larger than in Me_2S-OH, which is due to the better matching of ionization energies between OH (1.72 eV, DFT) and **1** (8.37 eV, DFT) than Me_2S (8.64 eV, DFT, 8.686 exptl[62]). The **1-OH** complex is also stabilized by an internal hydrogen bond. The O−H distance is 1.777 Å by B3LYP/6-31+G(d) and 1.750 Å by MP2/6-31+G(2d).

The radical complex **1-OH** can undergo a hydrogen transfer between the oxygen on the γ-carbon and the oxygen of the added OH. The product is a water complex of $CH_3SCH_2CH_2O$ (**2**). The transition state (**TS1−OH/2**) is relatively late as the forming O−H bond is much shorter than the breaking O−H bond (1.158/1.251 Å, DFT; 1.099/1.377 Å, MP2). The S−O bond in the transition state has lengthened 14% by DFT (2.381 → 2.722 Å) and 22% by MP2 (2.087 → 2.549 Å).

There is a significant difference between DFT and WF-1 activation enthalpies (Figure 2, $\Delta H^{\ddagger}$(298K) = 8.1 and 17.4 kcal/mol, respectively). Geometry optimization at the MP2/6-31+G(2d) level lowers the WF-1 activation barrier to 16.2 kcal/mol (Table 2). Since DFT is known to have difficulty describing 2c−3e bonding (as found in **1-OH**), it is likely that the actual barrier is 10−15 kcal/mol.

The product complex **2·H_2O** is 0.4 kcal/mol less stable than **1-OH** by DFT and 1.2 more stable than **1-OH** by WF-1. The water molecule is loosely bound to the $CH_3SCH_2CH_2O$ radical (binding ΔH(298K) = 1.9 and 2.0 kcal/mol by DFT and WF-1, respectively). The $CH_3SCH_2CH_2O$ radical (**2**) undergoes intramolecular hydrogen transfer from the methyl group to oxygen atom, thereby producing a carbon-centered radical (**3**), or undergoes carbon−carbon fragmentation to form formaldehyde and the CH_2SCH_3 radical. The former pathway has a lower activation enthalpy (5.4 versus 10.2 kcal/mol, Figure 1) and leads to more stable products (Figure 2).

The elimination of formaldehyde from **1-OH** has an analogy in the thermolysis of methyl ethyl sulfoxide where ethylene is eliminated (Figure 3). Jenks and co-worker[63] have recently

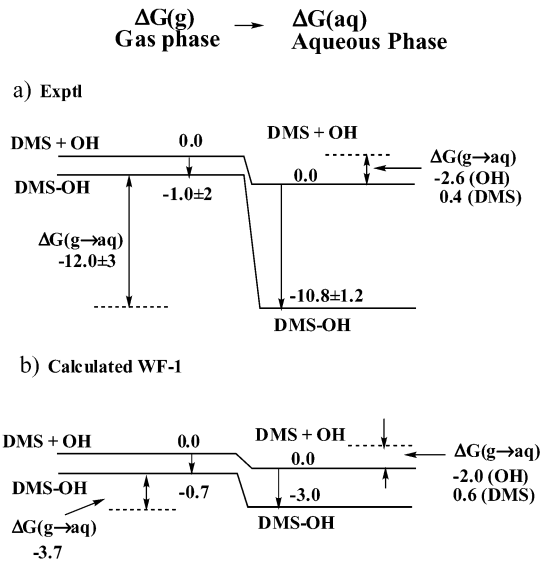

Figure 4. Thermochemical cycles showing the experimental (a) and computed (b) steps in the free energy of solvation of the DMS−OH 2c−3e adduct. The calculated solvation free energy of DMS−OH (ΔG(solv) = −3.7 kcal/mol) is significantly different from the experimental value[13] of −12.0 ± 3 kcal/mol.

studied the $CH_3S(O)CH_2CH_3 \rightarrow CH_3SOH + C_2H_4$ (eq 7) reaction and found it to be concerted. In a recent study of isomerization of the DMSO radical cation, Carlsen and Egsgaard[64] obtained the *aci*-DMSO radical cation through fragmentation of methyl carboxylmethyl sulfoxide cation which eliminates CO_2 (eq 8). It is not known whether the reaction is concerted or stepwise. In contrast, the radical reaction, **1-OH** → $H_2C{=}O + CH_2SCH_3 + H_2O$ (eq 9), is predicted to be stepwise (eq 10).

The **1-OH** complex can also fragment one of two C−S bonds (Figure 2). The BDE S−methyl is 19.0 kcal/mol (15.2 kcal/mol, WF-1) while the S−CH_2CH_2OH BDE is 18.9 kcal/mol (17.7 kcal/mol, WF-1). At the DFT level, the activation barrier for the S−C cleavage is 31.0 kcal/mol for the S−CH_3 bond and 29.1 kcal/mol for the S−CH_2CH_2OH bond. In the gas phase the lowest energy process for the **1-OH** complex is to lose OH (WF-1, endothermic by 12.2 kcal/mol) rather than migrate a hydrogen atom (WF-1, $\Delta H^{\ddagger}$(298K) = 17.4 kcal/mol). If MP2/6-31+G(2d) geometries are used, the WF-1 BDE of OH is 12.1 kcal/mol with an activation barrier of 16.1 kcal/mol for hydrogen migration (Table 2).

Aqueous Solution. The gas-phase reactions of OH with DMS are of direct relevance to understanding the chemistry of the atmosphere. In contrast, there is very little known about the gas-phase chemistry of OH plus 2-MTE, but extensive information is available on the aqueous solution-phase chemistry. While the computational results discussed above are probably accurate to 2−4 kcal/mol, the errors of the solution-phase results are more difficult to estimate.

The Gibbs free energy of solvation (ΔG(solv)) of DMS−OH was calculated by Merényi et al.[13] as −12 ± 3 kcal/mol from experimental data, which is in serious disagreement with the DFT value of −3.7 kcal/mol. A breakdown of the thermodynamic steps is given in Figure 4, where the standard state is mol/24.47 L in the gas phase and mol/L in solution. In their analysis, Merényi et al.[13] estimated the free energy of solvation from the S−O bond enthalpy in DMS−OH determined by Hynes et al. The experimental free energy of solvation (ΔG(solv)) for OH of −2.6 kcal/mol and of DMS of 0.4 kcal/mol are close to the values calculated in this study. As noted by Merényi et al., the value of −12 kcal/mol for ΔG(solv) of DMS−OH is "an usually large value for a neutral species".

TABLE 3: Comparison of Solution-Phase Redox and Acidity Parameters for DMS and 2-MTE

	X = DMS[a]	X = 2-MTE
redox[b] $X^{+\bullet}/X$	1.91 (1.66)[d]	1.66
redox[b] $X\therefore X^{+\bullet}/2X$	1.64 (1.40)	1.62
redox[b] X-OH/X + OH^-	1.53 (1.43)	1.39
acidity[c] $X^{+\bullet} + 2H_2O \rightleftarrows$ X-OH + H_3O^+	8.5	12.8
pK_a	6.2 (10.2)	9.4

[a] Experimental values are in parentheses. Reference 13. [b] Electromotive force (V) in aqueous solution at 298 K. The calculated EMF was determined relative to $\Delta G°$(298K) of the standard hydrogen electrode ($1/2H_2(g) \rightarrow H^+(aq)$; SHE) where the values $\Delta G°(1/2H_2(g) \rightarrow H(g)) = 48.58$ kcal/mol, $\Delta G°(H(g) \rightarrow H^+(g)) = 313.99$ kcal/mol, and $\Delta G°(H^+(g) \rightarrow H^+(aq)) = -262.4$ kcal/mol were taken from experiment or theory ($H^+(g) \rightarrow H^+(aq)$). [c] Free energy (kcal/mol) in aqueous solution at 298 K. [c] Also see: Engman, L.; Lind, J.; Merényi, G. *J. Phys. Chem.* **1994**, *98*, 3174.

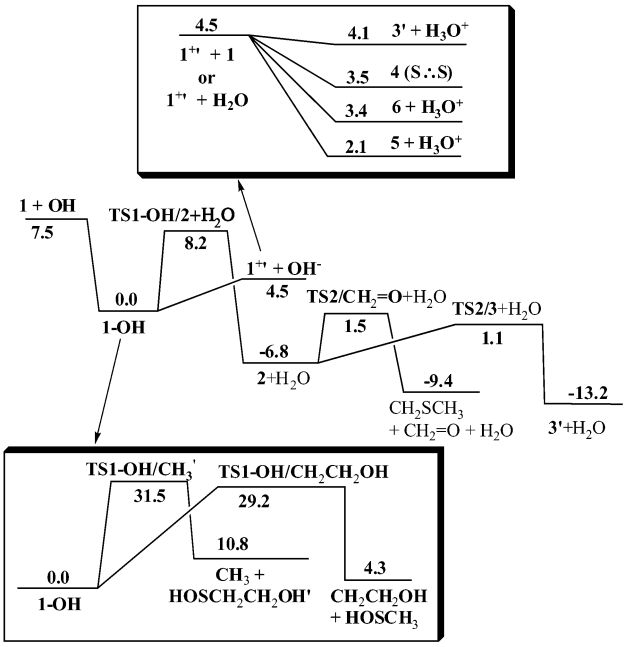

Figure 5. Reaction coordinate for OH + 2-MTE with solution free energies (298 K) at the B3LYP/6-31+G(d) level. The top box indicates the reactions of **1**$^{+\prime}$ with 2-MTE (**1**) to form the 2c−3e complex (**4**) or with H_2O to form **3′**, **5**, or **6**. The bottom box indicates the S−C cleavage reactions of **1-OH** to form CH_3/$HOSCH_2CH_2OH$ or CH_2CH_2-OH/$HOSCH_3$. The "prime" in the figure notation indicates that the conformer with the lowest free energy in solution is not the lowest energy conformer in the gas phase.

The redox potential, acidity, and pK_a are given for DMS and 2-MTE species in Table 3. The redox potential of $DMS^{+\bullet}$/DMS, $DMS\therefore DMS^{+\bullet}$/2DMS and DMS−OH/DMS + OH^-, which are known experimentally, are reproduced by theory to about 0.2 V. The corresponding redox potentials of 2-MTE are slightly smaller than the DMS values by about 0.2 V.

In aqueous solution, the free energy of the 2-MTE-OH adduct (**1-OH**) is 7.5 kcal/mol more negative than 2-MTE plus OH (Figure 5). When geometry optimization, including solvation at the CPCM/B3LYP/6-31+G(d) level, is made on the OH adduct of 2-MTE, the CPCM/B3LYP/6-31+G(d) energy is lowered by only 0.4 kcal/mol. The adduct can undergo homolytic cleavage to re-form 2-MTE and OH or undergo heterolytic cleavage to form $CH_3SCH_2CH_2OH^+$ plus OH^-. The free energy of $CH_3SCH_2CH_2OH^+/OH^-$ is only 4.5 kcal/mol (Figure 5) more positive than that of $CH_3S(OH)CH_2CH_2OH$

(**1-OH**). The activation free energy for internal hydrogen transfer is quite different, depending on whether the DFT (8.2 kcal/mol, Figure 5) or WF-1 (17.5 kcal/mol, Table 2) method is used to calculate the gas-phase free energy. In the complex, the S−O distances are 2.087 Å at MP2/6-31+G(2d) and 2.381 Å by B3LYP/6-31+G(d), which lengthen to 2.549 and 2.722 Å, respectively, in the transition state. The cause for the significant difference between the MP2 and DFT activation barriers (also mentioned in the preceding section) is probably attributable to the large difference in the optimized S−O distance in the MP2 and DFT transition states. In the DFT transition state geometry, the long S−O distance (2.722 Å) is probably an attractive interaction (or at least not as repulsive) by DFT but not by WF-1.

If CPCM/B3LYP/6-31+G(d) is used to optimize **TS1**−**OH**/**2**+H_2O, the DFT electronic barrier decreases by 3.2 kcal/mol (compared to using B3LYP/6-31+G(d) geometries). Thus, depending on the method, the free energy barrier is between about 5 and 15 kcal/mol. The effect of a catalytic water molecule was calculated on the **1-OH** → **2** + H_2O reaction (Figure 6). At the B3LYP/6-31+G(d) level, the activation enthalpy ($\Delta H^{\ddagger}$(g,298K)) was 5.5 kcal/mol, a slight reduction from the uncatalyzed reaction. When solvation and entropy effects are included, the H_2O-catalyzed reaction has a free energy of activation ($\Delta G^{\ddagger}$(aq,298K)) of 16.0 kcal/mol, an increase compared to the uncatalyzed reaction.

Under low pH conditions, an acid-catalyzed mechanism appears to be the most likely pathway between **1-OH** and **2** + H_2O. The first step is protonation of **1-OH** on the S−OH oxygen to give $CH_3SCH_2CH_2OH^+$ (**1**$^{+\prime}$) plus water that has a free energy of reaction of −12.8 kcal/mol (eq 10). The second step (eq 11), deprotonation of the terminal OH of SCH_2CH_2OH, has a free energy of 6.0 kcal/mol. The overall process (eq 12)

$$CH_3S(OH)CH_2CH_2OH + H_3O^+ \rightarrow CH_3SCH_2CH_2OH^+ + 2H_2O \quad \Delta G^\circ_{rxn} = -12.8 \quad (10)$$

$$CH_3SCH_2CH_2OH^+ + H_2O \rightarrow CH_3SCH_2CH_2O + H_3O^+ \quad \Delta G^\circ_{rxn} = 6.0 \quad (11)$$

$$\text{Net: } CH_3S(OH)CH_2CH_2OH \rightarrow CH_3SCH_2CH_2O + H_2O \quad \Delta G^\circ_{rxn} = -6.8 \quad (12)$$

is spontaneous by −6.8 kcal/mol. From the $CH_3SCH_2CH_2O$ intermediate (**2**), the oxygen can abstract a hydrogen to form $CH_2SCH_2CH_2OH$ (**3**′) with $\Delta G^{\ddagger}$(298K) = 7.9 kcal/mol. Alternatively, the $CH_3SCH_2CH_2O$ (**2**) can cleave at the C−C bond to form CH_2SCH_3 plus $CH_2{=}O$ with $\Delta G^{\ddagger}$(298K) = 8.3 kcal/mol (Figure 5).

The experimental results[21] indicate that approximately half of the hydroxyl radicals that add to 2-MTE (**1**) result in formaldehyde. The activation free energy for forming $CH_2SCH_2CH_2OH$ (**3**′) is a little lower than for forming formaldehyde. On the other hand, the **2** → **3**′ reaction is reversible to a greater extent than the reaction **2** → formaldehyde + CH_2SCH_3, since the reverse reaction is unimolecular in the former reaction and bimolecular in the latter reaction.

If the **1-OH** adduct undergoes heterolytic cleavage, the $CH_3SCH_2CH_2OH^+$ cation can eliminate a C−H proton to form one of three possible neutral radicals: $CH_3SCH_2{}^{\bullet}CHOH$ (**5**), $CH_3S{}^{\bullet}CHCH_2OH$ (**6**), or $^{\bullet}CH_2SCH_2CH_2OH$ (**3**′), which correspond to loss of a proton from the α-carbon, *β*-carbon, or methyl carbon, respectively. Experimental ESR evidence in aqueous solution[65] suggests that more than one radical can be formed by the deprotonation of **1**$^+$. The present study indicates that **3**′, **5**, and **6** are all within 2.0 kcal/mol of each other in free energy (Figure 5). Alternatively, the **1**$^{+\prime}$ cation can associate with **1** to form the symmetrical 2c−3e bonded complex (**4**), where the calculated sulfur−sulfur bond in the complex (^2A_u state) is 2.951 Å. The $(S\therefore S)^+$ complex (**4**) is not observed at pH > 2 in the OH-induced oxidation of 2-MTE, but it is when the triplet state of 4-carboxybenzophenone is quenched by 2-MTE.[21,22] The explanation put forth by Schöneich and coworkers, and supported by the present calculations, is that **1-OH** undergoes faster conversion into **2** (acid/base-catalyzed proton transfer) than electron transfer to **1**$^+$.

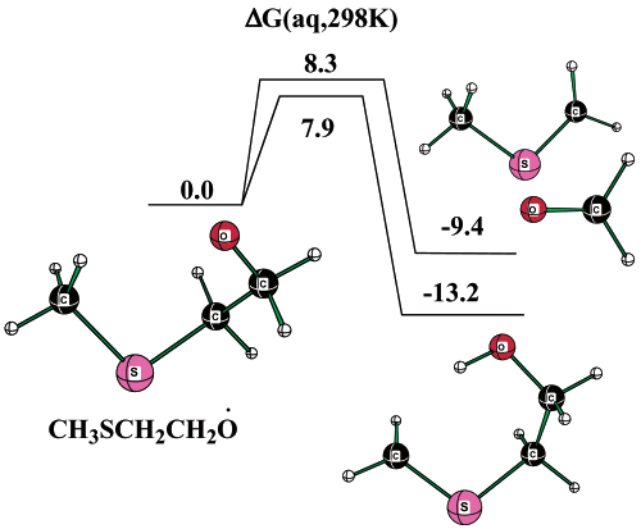

Figure 6. Enthalpies (ΔH(g,298K)) and free energies ((ΔG(aq,298K)) for the conversion of **1-OH** to **2** + H_2O catalyzed by one water molecule. Geometries were calculated at the B3LYP/6-31+G(d) level. While the enthalpy of activation of the catalyzed reaction in the gas phase is lower in energy then the uncatalyzed reaction, the free energy of activation of the catalyzed reaction in solution is higher in free energy than the uncatalyzed reaction.

At high pH, eq 13

$$\textbf{1-OH} + OH^- \rightarrow \textbf{2} + OH^- + H_2O \quad \Delta G^\circ_{rxn} = -6.8 \quad (13)$$

is predicted to dominate. If a hydroxide anion abstracts a proton from the OH group attached to the *β*-carbon of **2**, the gas-phase B3LYP/6-31+G(d) optimization of $CH_3S(OH)CH_2CH_2O^-$ yields a hydrogen-bonded complex between **2** and OH^-.

4. Conclusions

The oxidation of two sulfides, DMS (CH_3SCH_3) and 2-MTE ($CH_3SCH_2CH_2OH$), has been studied by computational methods in the gas and solution phases. The initial OH-adduct is an unsymmetrical S∴O 2c−3e interaction that is not properly described at either the B3LYP or MP2 level of theory. The B3LYP method predicts the S−O distance to be much longer than the MP2 method. Using the composite method, WF-1, which is very similar to the G2(MP2,SVP) procedure, the DFT geometry gives a slightly lower energy than the MP2 geometry. However, DFT (B3LYP/6-31+G(d)) gives OH binding energies which are too large by about 3 or 4 kcal/mol.

Solvation effects are computed by combining the gas-phase free energy (298 K) with the solvation free energy (ΔG(solv)) computed using the CPCM method on fixed gas-phase geometries. In many cases, the conformer with the lowest free energies is different in the gas and solution phase. The gas phase favors structures with an internal hydrogen bond, while solution

phase favors more open structures. The oxidation of 2-MTE proceeds with a competition between electron transfer to form OH^- and $CH_3SCH_2CH_2OH^+$ (**1**$^+$) and the acid-/base-catalyzed formation of $CH_3SCH_2CH_2O$ (**2**) + H_2O. The concerted or one-water catalyzed transformations of the OH-adduct (**1-OH**) to **2** + H_2O have significant free energies of activation. From **2**, the internal hydrogen transfer to form $CH_2SCH_2CH_2OH$ (**3′**) and the fragmentation to CH_2SCH_3 + $H_2C{=}O$ have very similar free energy barriers (7.9 and 8.3 kcal/mol). The cation of 2-MTE (**1**$^+$) can associate with a neutral 2-MTE molecule to form the symmetrical 2c−3e S∴S bonded system (**4**) in a reaction that has a negative free energy change (−1.0 kcal/mol). In addition, **1**$^+$ can lose a C−H proton to form three difference radicals, all of which have similar free energies.

To summarize, in aqueous solution the adduct between 2-MTE and hydroxyl radical is predicted to undergo an acid-catalyzed conversion to $CH_3SCH_2CH_2O$ (**2**) plus water where **2** can further fragment to formaldehyde or rearrange to $CH_2SCH_2CH_2OH$ (**3′**). In competition with this process, **2** can be oxidized to the cation and can associate with **2** to form a S∴S 2c−3e complex (**4**) or lose a C−H proton (**3′**, **5**, or **6**). While it is clear that these pathways should have different pH dependences, computing the branch ratio is not possible given the uncertainty in the rate of the acid-catalyzed reaction. There is, however, experimental evidence that these processes are competitive.

Acknowledgment. Computer time was provided by the Alabama Supercomputer Network, the Maui High Performance Computer Center, and the Auburn COSAM PRISM cluster.

Supporting Information Available: Absolute energies for species in Table 1 (Table S1) and Cartesian coordinates for relevant structures optimized at the B3LYP/6-31+G(d) or MP2/6-31+G(2d) level of theory (Table S2). This material is available free of charge via the Internet at http://pubs.acs.org.

References and Notes

(1) Williams, M. B.; Campuzano-Jost, P.; Bauer, D.; Hynes, A. J. *Chem. Phys. Lett.* **2001**, *344*, 61.

(2) Arsene, C.; Barnes, I.; Becker, K. H. *Phys. Chem. Chem. Phys.* **1999**, *1*, 5463.

(3) Butkovskaya, N. I.; Setser, D. W. *J. Phys. Chem. A* **1998**, *102*, 6395.

(4) Silvente, E.; Richter, R. C.; Hynes, A. J. *J. Chem. Soc., Faraday Trans.* **1997**, *93*, 2821.

(5) Silvente, E.; Richter, R. C.; Hynes, A. J. *J. Chem. Soc., Faraday Trans.* **1997**, *93*, 2821.

(6) Hynes, A. J. Reaction Mechanisms in Atmospheric Chemistry: Kinetic Studies of Hydroxyl Radical Mechanisms. In *Spectroscopy in Environmental Sciences;* Clark, R. J. H., Hester, R. E., Eds.; Wiley & Sons: New York, 1995.

(7) Hynes, A. J.; Stoker, R. B.; Pounds, A. J.; McKay, T.; Bradshaw, J. D.; Nicovich, J. M.; Wine, P. H. *J. Phys. Chem.* **1995**, *99*, 16967.

(8) Stickel, R. E.; Zhao, Z.; Wine, P. H. *Chem. Phys. Lett.* **1993**, *212*, 312.

(9) (a) Asmus, K.-D. *Nukleonika* **2000**, *45*, 3. (a) Asmus, K.-D. In *Sulfur-Centered Reactive Intermediates in Chemistry and Biology*; Chatgilialoglu, C., Asmus, K.-D., Eds.; Plenum Press: New York and London, 1990; p 155.

(10) Gawandi, V. B.; Mohan, H.; Mittal, J. P. *J. Chem. Soc., Perkin Trans. 2* **1999**, 1425.

(11) Gawandi, V. B.; Mohan, H.; Mittal, J. P. *Chem. Phys. Lett.* **1999**, *314*, 451.

(12) Schöneich, C.; Asmus, K.-D. *J. Am. Chem. Soc.* **1993**, *115*, 11376.

(13) Merényi, G.; Lind, J.; Engman, L. *J. Phys. Chem.* **1996**, *100*, 8875.

(14) Pogocki, D.; Schöneich, C. *J. Org. Chem.* **2002**, *67*, 1526.

(15) Pogocki, D.; Ghezzo-Schöneich, E.; Schöneich, C. *J. Phys. Chem. B* **2001**, *105*, 1250.

(16) Schöneich, C.; Miller, B.; Hug, G. L.; Bobrowski, K.; Marciniak, B. *Res. Chem. Intermed.* **2001**, *27*, 165.

(17) Bonifačić, M.; Hug, G. L.; Schöneich, C. *J. Phys. Chem. A* **2000**, *102*, 1240.

(18) Schöneich, C.; Pogocki, D.; Wisniowski, P.; Hug, G. L.; Bobrowski, K. *J. Am. Chem. Soc.* **2000**, *122*, 10224.

(19) (a) Bobrowski, K.; Hug, G. L.; Marciniak, B.; Miller, B.; Schöneich, C. *J. Am. Chem. Soc.* **1997**, *119*, 8000. (b) Bobrowski, K.; Pogocki, D.; Schoneich, C. *J. Phys. Chem. A* **1998**, *102*, 10512.

(20) Steffen, L. K.; Glass, R. S.; Sabahi, M.; Wilson, G. S.; Schöneich, C.; Mahling, S.; Asmus, K. D. *J. Am. Chem. Soc.* **1991**, *113*, 2141.

(21) Bobrowski, K.; Hug, G. L.; Marciniak, B.; Miller, B.; Schöneich, C. *J. Am. Chem. Soc.* **1997**, *119*, 8000.

(22) Schöneich, C.; Bobrowski, K. *J. Am. Chem. Soc.* **1993**, *115*, 6538.

(23) Wang, L.; Zhang, *J. Chem. Phys. Lett.* **2002**, *356*, 490.

(24) Frisch, M. J.; Trucks, G. W.; Schlegel, H. B.; Scuseria, G. E.; Robb, M. A.; Cheeseman, J. R.; Zakrzewski, V. G.; Montgomery, Jr., J. A.; Stratmann, R. E.; Burant, J. C.; Dapprich, S.; Millam, J. M.; Daniels, A. D.; Kudin, K. N.; Strain, M. C.; Farkas, O.; Tomasi, J.; Barone, V.; Cossi, M.; Cammi, R.; Mennucci, B.; Pomelli, C.; Adamo, C.; Clifford, S.; Ochterski, J.; Petersson, G. A.; Ayala, P. Y.; Cui, Q.; Morokuma, K.; Malick, D. K.; Rabuck, A. D.; Raghavachari, K.; Foresman, J. B.; Cioslowski, J.; Ortiz, J. V.; Stefanov, B. B.; Liu, G.; Liashenko, A.; Piskorz, P.; Komaromi, I.; Gomperts, R.; Martin, R. L.; Fox, D. J.; Keith, T.; Al-Laham, M. A.; Peng, C. Y.; Nanayakkara, A.; Gonzalez, C.; Challacombe, M.; Gill, P. M. W.; Johnson, B.; Chen, W.; Wong, M. W.; Andres, J. L.; Gonzalez, C.; Head-Gordon, M.; Replogle, E. S.; and Pople, J. A. *Guassian 98* (revision A.6); Gaussian, Inc.: Pittsburgh, PA, 1998.

(25) Koch, W.; Holthausen, M. C. *A Chemist's Guide to Density Functional Theory*; Wiley-VCH: New York, 2000.

(26) Byrd, B. F. C.; Sherrill, C. D.; Head-Gordon, M. *J. Phys. Chem. A* **2001**, *105*, 9736.

(27) Schaftenaar, G.; Noordik, J. H. Molden: A pre- and post-processing program for molecular and electronic structures. *J. Comput.-Aided Mol. Design* **2000**, *14*, 123.

(28) (a) McKee, M. L.; Lipscomb, W. N. *J. Am. Chem. Soc.* **1981**, *103*, 4673. (b) Nobes, R. H.; Bouma, W. J.; Radom, L. *Chem. Phys. Lett.* **1982**, *89*, 497. (c) McKee, M. L.; Lipscomb, W. N. *Inorg. Chem.* **1985**, *24*, 762.

(29) (a) Smith, B. J.; Radom, L. *J. Phys. Chem.* **1995**, *99*, 6468. (b) Curtiss, L. A.; Redfern, P. C.; Smith, B. J.; Radom, L. *J. Chem. Phys.* **1996**, *104*, 5148. (c) Nicolaides, A.; Rauk, A.; Glukhovtsev, M. N.; Radom, L. *J. Phys. Chem.* **1996**, *100*, 17460.

(30) Braïda, B.; Hazebroucq, S.; Hiberty, P. C. *J. Am. Chem. Soc.* **2002**, *124*, 2371.

(31) Chermette, H.; Ciofini, I.; Mariotti, F.; Daul, C. *J. Chem. Phys.* **2001**, *115*, 11068.

(32) Braïda, B.; Lauvergnat, D.; Hiberty, P. C. *J. Chem. Phys.* **2001**, *115*, 90.

(33) Braïda, B.; Hiberty, P. C. *J. Phys. Chem. A* **2000**, *104*, 4618.

(34) Braïda, B.; Thogersen, L.; Wu, W.; Hiberty, P. C. *J. Am. Chem. Soc.* **2002**, *124*, 11781.

(35) Bally, T.; Sastry G. N. *J. Phys. Chem. A* **1997**, *101*, 7923.

(36) Braïda, B.; Hiberty, P. C.; Savin, A. *J. Phys. Chem. A* **1998**, *102*, 7872.

(37) Sodupe, M.; Bertran, J.; Rodriguez-Santiago, L.; Baerends, E. J. *J. Phys. Chem A* **1999**, *103*, 166.

(38) CPCM is a conductor-like screening solvation model (COSMO) with a continuum polarizable description of solvent that takes into account both electrostatic and van der Waals contributions. Solvation energies were estimated for water (ϵ = 78.39). (a) Cossi, M.; Scalmani, G.; Rega, N.; Barone, V. *J. Chem. Phys.* **2002**, *117*, 43. (b) Barone, V.; Cossi, M. *J. Phys. Chem. A* **1998**, *102*, 1995. (c) Barone, B.; Cossi, M.; Tomasi, J. *J. Comput. Chem.* **1998**, *19*, 404.

(39) Smith, B. J. *Phys. Chem. Chem. Phys.* **2002**, *2*, 5383.

(40) Tomasi, J.; Cammi, R.; Mennucci, B. *Int. J. Quan. Chem.* **1999**, *75*, 783.

(41) Amovilli, C.; Barone, V.; Cammi, R.; Cancès, E.; Cossi, M.; Mennucci, B.; Pomelli, C. S.; Tomasi, J. *Adv. Quantum Chem.* **1999**, *32*, 227.

(42) (a) Cramer, C. J. *Essentials of Computational Chemistry: Theories and Models*; Wiley: Chichester, UK, 2002. (b) Cramer, C. J.; Truhlar, D. G. *Chem. Rev.* **1999**, *99*, 2161.

(43) Pliego, Jr., J. R.; Riveros, J. M. *Phys. Chem. Chem. Phys.* **2002**, *4*, 1622.

(44) Li, H.; Hains, A. W.; Everts, J. E.; Robertson, A. D.; Jensen, J. H. *J. Phys. Chem. B* **2002**, *106*, 3486. (b) Liptak, M. D.; Shields, G. C. *J. Am. Chem. Soc.* **2001**, *123*, 7314.

(45) Zhan, C.-G.; Dixon, D. A. *J. Phys. Chem. A* **2001**, *105*, 11534.

(46) (a) Zhan, C.-G.; Dixon, D. A. *J. Phys. Chem. A* **2002**, *106*, 9737. (b).

(47) *CRC Handbook of Chemistry and Physics*, 83rd ed.; Lide, D. R., Ed.; CRC Press: Boca Raton, FL, 2002.

(48) (a) Poskrebyshev, G. A.; Neta, P.; Huie, R. E. *J. Phys. Chem. A* **2002**, *106*, 11488. (b) Stanbury, D. M. *Adv. Inorg. Chem.* **1989**, *33*, 69.

(49) A similar value of $\Delta G(\text{solv}) = -2.4$ kcal/mol for OH is reported. Schwarz, H. A.; Dodson, R. W. *J. Phys. Chem*. **1984**, *88*, 3643.

(50) McKee, M. L. *J. Phys. Chem.* **1993**, *97*, 10971.

(51) Tureček, F. *Collect. Czech. Chem. Commun.* **2000**, *65*, 455.

(52) Wang, L.; Zhang, J. *THEOCHEM* **2001**, *543*, 167.

(53) Tureček, F. *J. Phys. Chem.* **1994**, *98*, 3701.

(54) Gu, M.; Turecek, F. *J. Am. Chem. Soc*. **1992**, *114*, 7146.

(55) Maity, D. K. *J. Phys. Chem. A* **2002**, *106*, 5716.

(56) Bickelhaupt, F. M.; Diefenbach, A.; De Visser, S. P.; De Koning, L. J.; Nibbbering, N. M. M. *J. Phys. Chem. A* **1998**, *102*, 9549.

(57) De Visser, S. P.; Bickelhaupt, F. M.; De Koning, L. J.; Nibbering, N. M. M. *Int. J. Mass Spectrom. Ion Processes* **1998**, *179/180*, 43.

(58) The MP2 method systematically underestimates the 2c−3e bond distance (see ref 33).

(59) McKee, M. L.; Wine, P. H. *J. Am. Chem. Soc.* **2001**, *123*, 2344.

(60) Marstokk, K.-M.; Møllendal, H.; Uggerud, E. *Acta Chem. Scand.* **1989**, *43*, 26.

(61) The average S--H hydrogen bond distance is 1.9−2.0 Å; See: Steiner, T. *Chem. Commun*. **1998**, 411.

(62) Limão-Vieira, P.; Eden, S.; Kendall, P. A.; Mason, N. J. Hoffmann, S. V. *Chem. Phys. Lett.* **2002**, *366*, 343.

(63) Cubbage, J. W.; Guo, Y.; McCulla, R. D.; Jenks, W. S. *J. Org. Chem.* **2001**, *66*, 8722.

(64) Carlsen, L.; Egsgaard, H. *J. Am. Chem. Soc.* **1988**, *110*, 6701.

(65) (a) Gilbert, B. C.; Larkin, J. P.; Norman, R. O. C. *J. Chem. Soc., Perkin 2* **1973**, 273. (b) Gilbert, B. C.; Hodgeman, D. K. C.; Norman, R. O. C. *J. Chem. Soc., Perkin 2* **1973**, 1748.